Transportation Geotechnics 20 (2019) 100240

Contents lists available at ScienceDirect

Transportation Geotechnics

journal homepage: www.elsevier.com/locate/trgeo

Analysis of geometric ballast plate for laboratory testing of resilient track components

Jacob M. Branson*, Marcus S. Dersch, Arthur de Oliveira Lima, J. Riley Edwards, Jae-Yoon Kim

Rail Transportation and Engineering Center – RailTEC, Department of Civil and Environmental Engineering – CEE, University of Illinois at Urbana-Champaign – UIUC, 205 N. Mathews Ave., MC-250, B118 Newmark Civil Engineering Laboratory, Urbana, IL 61801, United States

ARTICLE INFO

Keywords:
Under tie pads
Railroad ballast
Matrix based tactile surface sensors
Pressure distribution
3D scanning
Geometric ballast plate

ABSTRACT

Under tie pads (UTPs) have become a common solution for railroad networks across the world to improve track quality and reduce maintenance. Despite the benefits of UTPs in heavy-haul applications, there are currently no testing standards pertaining to UTPs in high axle load environments. The current European standard, the EN 16730:2016, recommends the use of a geometric ballast plate (GBP) in place of actual ballast for several tests. The GBP's lightweight construction and geometric design allows for ease of use and repeatability in laboratory testing. However, GBP and ballast contact with UTPs have not been thoroughly documented within the literature. Therefore, this study aims to compare the relationship between GBP and ballast contact surfaces through a variety of laboratory tests and 3D scanning. Several ballast "blocks" were cast to serve as repeatable ballast specimens for the tests and scans. Top contact surface, pressure distribution characteristics, and geometric properties of the GBP and ballast blocks were compared. Results showed that the GBP generally overestimates the contact characteristics of ballast, resulting in lower pressures, higher contact areas, greater total areas at given depths, and smaller particle spacing than the ballast blocks. Using these results, a more realistic GBP design can be developed. This work will be valuable in establishing more accurate testing methods/support conditions to enable representative, easy, and repeatable laboratory testing of resilient track components.

Introduction

Under tie pads (UTPs) have emerged as a solution for railway systems to improve track quality and reduce environmental impact. Implementation of UTPs has increased due to their effectiveness at preserving ballast and maintaining proper alignment [24]. By conforming to ballast particles to more evenly distribute loads and avoiding point contact between the crosstie and ballast, UTPs reduce the stress state at the crosstie-ballast interface and mitigate detrimental effects from impact loads [13,12,14,21]. Ultimately, this can result in an extension of ballast maintenance cycles and a subsequent reduction in track maintenance costs. In addition, UTP installations have shown potential environmental benefits by reducing the effects of ground-borne vibrations on nearby structures [15,19]. For these reasons, UTPs have been adopted as a standard component on several European rail networks and are being implemented in specialized locations in North and South America, Australia, and Asia [24,14,21].

The emergence of UTPs in heavy-haul railway applications has led to the need for adequate testing protocols. Currently, the prevailing standards for testing UTPs are outlined in the European standard EN 16730:2016 (hereafter referred to as the "EN") [7]. The EN outlines a variety of UTP tests that focus on the quantification of bedding modulus, environmental effects, fatigue performance, etc. These tests are designed for UTP use in Europe and not the heavy axle load (HAL) freight railroad operating environment typical of North America [16].

For several tests, the EN recommends the use of a geometric ballast plate (GBP) in lieu of ballast as a loading surface for the UTP during laboratory testing [7]. The GBP is a profiled steel plate containing several raised nodes arranged in a symmetric grid designed to replicate the contact of ballast particles (Fig. 1). Three different node designs are used for the GBP's surface, the larger with 46 mm (1.81 in.) sides and the smaller two with 21 mm (0.87 in.) sides and differing top surface areas. The rigid and geometric design of the GBP reduces the intrinsic variability associated with actual ballast by providing a consistent support condition for specimens regardless of orientation [17]. In addition, the GBP is relatively lightweight, making for easier handling during test setup than ballast. The EN GBP was designed to replicate an earlier design of a ballast plate constructed for testing under ballast mat

* Corresponding author.
E-mail addresses: jbranso2@illinois.edu (J.M. Branson), mdersch2@illinois.edu (M.S. Dersch), aolima@illinois.edu (A. de Oliveira Lima), jedward2@illinois.edu (J.R. Edwards), jaeyoon4@illinois.edu (J.-Y. Kim).

https://doi.org/10.1016/j.trgeo.2019.04.003
Received 5 December 2018; Received in revised form 26 April 2019; Accepted 26 April 2019
Available online 27 April 2019
2214-3912/ Published by Elsevier Ltd.

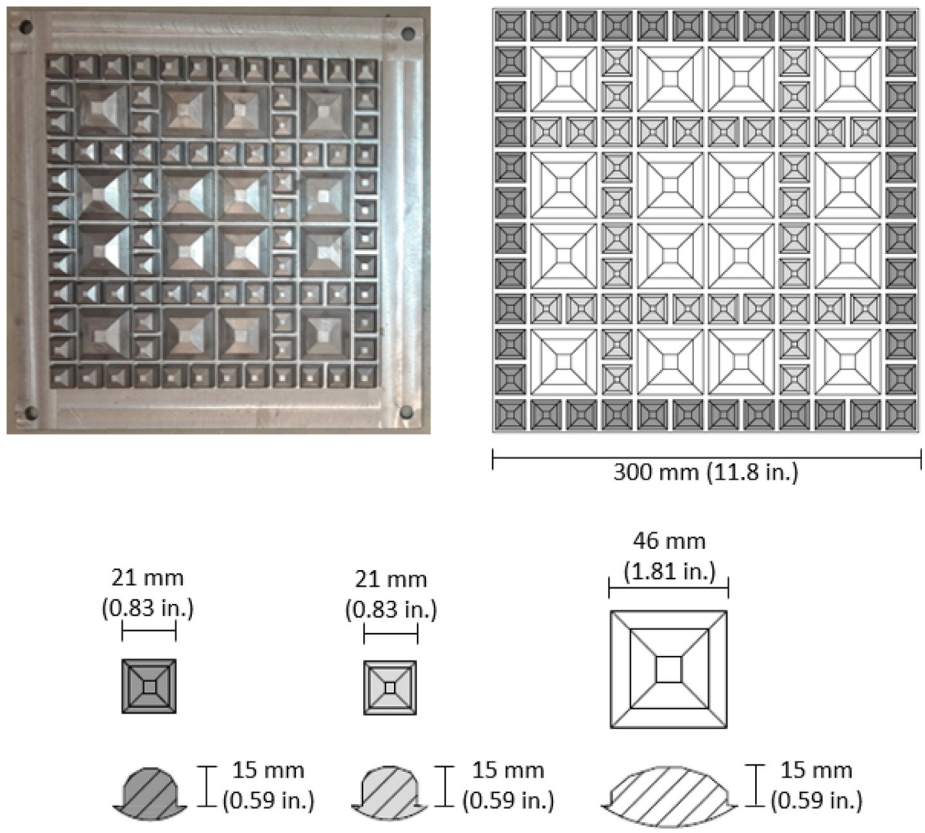

Fig. 1. Geometric ballast plate per specifications of the EN 16730:2016 standard, including details of nodes.

products according to the German Deutsches Institut für Normung (DIN) standard [24,6]. To date, the authors of this paper have discovered no research to verify that the GBP is an adequate substitute for actual ballast.

Given the contact properties of ballast and GBP with UTPs are unknown, a series of tests were performed to compare the GBP's contact surface performance against actual ballast. Ballast "blocks" were designed and manufactured to provide repeatable test specimens representing actual ballast support/contact conditions. Direct contact comparisons between the ballast blocks and GBP were made through top surface contact tests. Additionally, both support conditions were tested in a series of pressure distribution tests with multiple UTP products to compare how the GBP and ballast affected the results as the components conformed to their unique surfaces. Finally, both qualitative and quantitative comparisons were made through 3-dimensional (3D) scanning of the GBP and ballast blocks. Data from all three types of tests can be used to improve the design of the GBP to make it more representative of actual ballast surface contact conditions.

Material and methods

Ballast blocks

Four 305 mm × 305 mm × 102 mm (12″ × 12″ × 4″) ballast blocks were constructed to provide repeatable and manageable specimens representative of actual ballast contact conditions. The size of the blocks was selected to be similar to that of the GBP. Each block comprised of ballast meeting AREMA Grade 4A specifications and a two-part polyurethane product designed for bonding railroad ballast [4,2]. Grade 4A ballast is a common ballast gradation used in North America and it was chosen since it is representative of typical ballast. Fig. 2 shows the steps followed for manufacture of the ballast blocks. The procedure started by mixing ballast in a bucket with enough epoxy to ensure adequate coating of all particles, as shown in step (a). The coated ballast was then poured into a form to create the rough shape of the ballast block (b). Before the epoxy set, a steel plate was set over the top surface of the ballast and the setup was compacted for one minute using a vibratory compactor (c). This compaction was performed to represent the condition of in-service ballast that has been subjected to loading under a crosstie. Previous research from Lima [18] indicates that 60 s of similar compaction techniques result in a ballast density of around 0.62 lbs/in^3 (17.1 g/cm^3), which is comparable to field ballast density [25]. Once the epoxy cured and the block was removed from the form, a 2.54 mm (1 in.) layer of gypsum cement was applied to the bottom surface of the blocks to create a level base surface to minimize eccentricities during loading (d). The first three finished blocks were labeled BB1-BB3 and are collectively referenced as the "standard blocks" in this paper. The standard blocks were constructed using the same construction method to provide a baseline contact surface representing clean ballast. To provide variability in the blocks and investigate the effect of non-uniform ballast surface profiles, one block (designated BBM1) was modified to represent an uneven contact condition by rotating/raising some of the particles near the surface by hand after vibration was performed.

Laboratory testing

Loading for each test was applied using a hydraulic vertical actuator with a flat steel plate mounted to the actuator head. Matrix based tactile surface sensors (MBTSS) were used for tests in which determination of contact area and pressure distribution were desired outputs. MBTSS use a grid of semi-conductive ink to determine the magnitude and location of contact pressures between two objects in contact. The grid design of the MBTSS creates 1936 individual points—called sensels—each of 12.29 mm^2 (0.0484 in^2) to measure contact pressure [22]. Due to the thin construction of MBTSS, the sensors used during these tests were

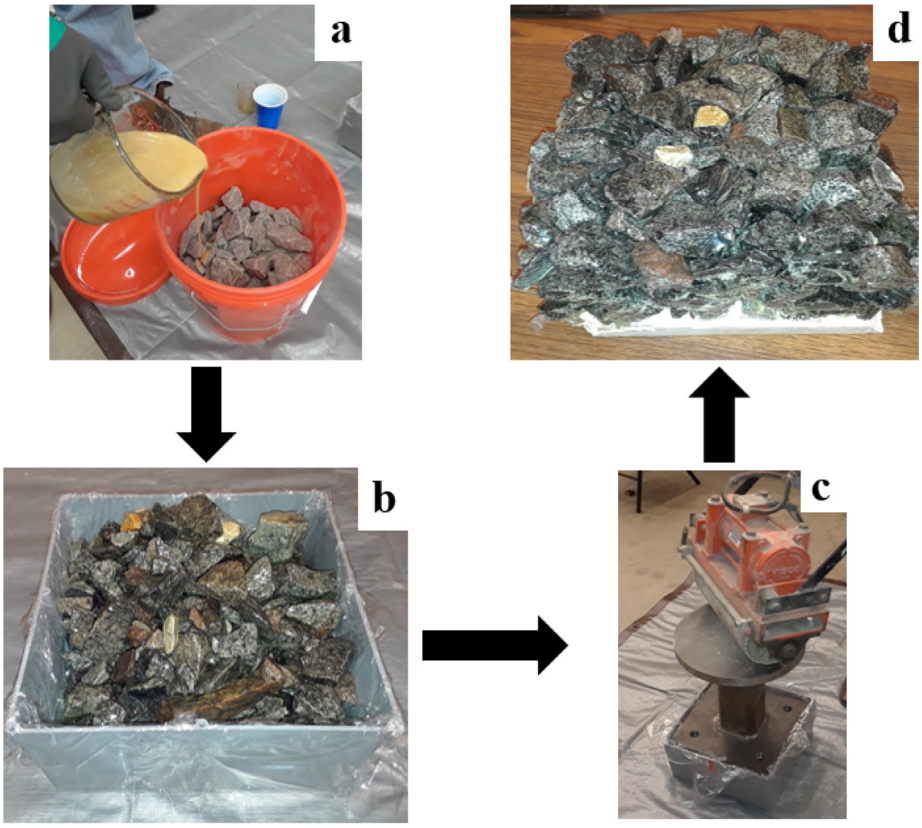

Fig. 2. Ballast block construction steps; (a) epoxy pouring, (b) forming, (c) compaction, and (d) finished product with gypsum cement base.

outfitted with layers of polytetrafluoroethylene (PTFE) and biaxially-oriented polyethylene terephthalate (BoPET) to protect them from shear and puncture damage [22,26,10]. In railroad research, MBTSS have been utilized to measure pressures between crosstie plates and crossties [23,26], crossties and ballast [20,9], and within the railseat [22,10,11].

For top surface contact tests, loads were directly applied to the GBP and ballast blocks through a 203 mm × 203 mm (8″ × 8″) flat steel plate placed on the surface of the support condition. An MBTSS was placed between the steel plate and the support condition to measure the contact area between the two surfaces. A diagram of the test setup is provided in Fig. 3(a). This test provides a baseline contact value to compare each support condition and is useful for analyzing how each interacts with a flat surface, such as a concrete crosstie. The surface area results within this paper are given as a percentage of the total area subject to loading, or 41,290 mm^2 (64 in^2) for these tests.

While surface contact is an important metric to consider, it is not the only characteristic that defines a support condition. UTPs are effective in pressure mitigation because they conform to the ballast particles and distribute loads over a greater area [12]. As a result, pressure distribution should be considered when designing a representative support condition. To quantify the UTP's effectiveness at mitigating pressures, MBTSS were employed to quantify pressure distribution through two different types of UTP products, one made from rubber and one from polyurethane foam. Fig. 3(b) shows a diagram of the test setup for both types of support. Four specimens of each UTP type were tested on each of the four ballast blocks and on the GBP. The test procedure followed the EN's static bedding modulus test, with four cycles to precondition the specimens and one cycle to collect the data. To account for higher axle loads associated with heavy-haul environments, the load

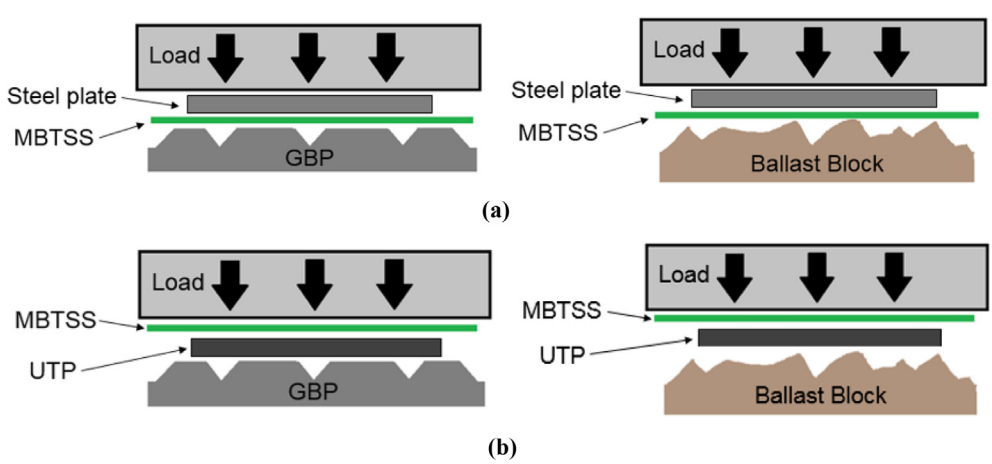

Fig. 3. Test setup of top surface contact tests (a), and pressure distribution tests (b) for each support condition.

magnitudes outlined in the EN were raised to represent the 95th percentile nominal axle load for HAL freight operations, specified by AREMA as 356 kN (80 kips) [16,1]. Three primary metrics—maximum pressure, average pressure, and contact area—were determined from each test. Average pressure indicates the mean pressure magnitude over all loaded sensels for each test and is useful in analyzing how the pressure is distributed within each support condition. Contact area is the sum of the areas of all loaded sensels.

3D Scanning

To form a comprehensive understanding of the geometry of the ballast blocks, each block was scanned and converted into a 3D model to determine geometrical metrics useful for creating a revised GBP. A Steinbichler scanner programmed with Colid3D software was used to capture the scans. This particular scanner model scanned with a 1600 × 1200 resolution with a minimum point placement accuracy of 0.25 mm (0.01 in.). The master files for each block were comprised of around twenty scans, each from a different angle around the top surface to capture data on all sides and surfaces of the block. Since contact between the UTP and the top layer of ballast is the focus of this study, only the top 25 mm (~1 in.) of each block was scanned and processed. The scanning setup and corresponding 3D model representation of a ballast block are shown in Fig. 4. After scanning was complete, the master files for each scan were refined and holes in the scans were patched using post-processing software [5]. Further post-processing and analysis of the master data files were performed in a variety of computer aided design (CAD) software applications to determine contour lines, cross sectional areas, and average particle spacing.

Several geometric features of the ballast blocks were quantified using the scan data. To measure the contact surfaces at various elevations from the top of each block, contour plots were created in CAD software at 1 mm elevation intervals by bisecting the block scans with a horizontal plane at each elevation. The intersection between each plane and the edges of the particles formed the contour lines. The resulting areas from within each contour circle were used to measure the average size of each particle at the given elevation and an approximation of total amount of contact at that elevation for each block. In addition, the average particle spacing in each block was determined by taking the average distance between adjacent particles using the process of Delaunay triangulation. Delaunay triangulation determines the distances between points using an algorithm that draws triangles with circumcircles that have no other points within them [3,8]. The geometric centers of the particles at 5 mm were used to represent each particle. To minimize the influence of particle spacing from the form, only particles with geometric centers falling within an interior 200 mm × 200 mm (8″ × 8″) square were analyzed (Fig. 5).

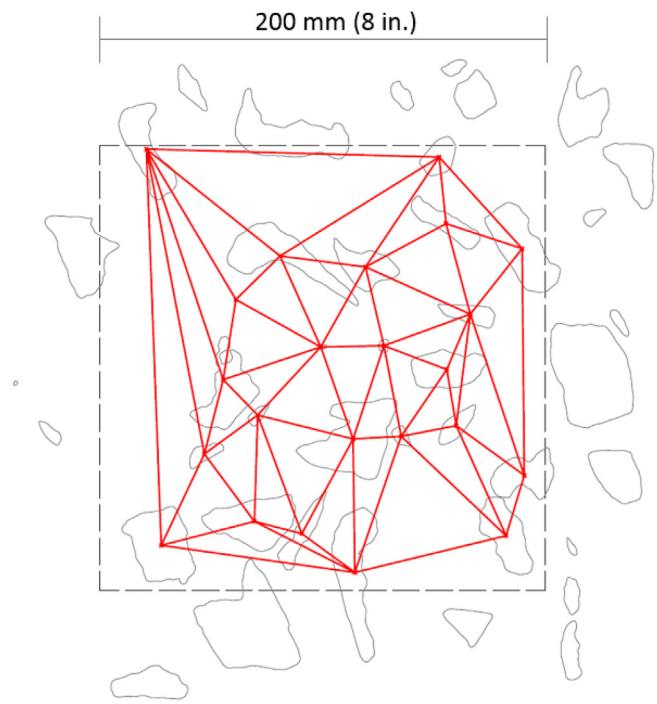

Fig. 5. Representative schematic of Delaunay triangulation as performed on ballast blocks to determine particle spacing at a depth of 5 mm.

Results and discussion

Top surface contact tests

Qualitative and quantitative results from the top surface contact tests are illustrated in Fig. 6. The GBP resulted in the highest contact area of all support conditions with approximately 7 percent of total area (PTA). The ballast blocks resulted in less contact, all falling within 3.3 and 4.8 PTA. Thus, the GBP resulted in contact areas 1.4 to 2.1 times higher than the ballast blocks. The mean composite contact area value for all ballast blocks resulted in approximately 4 PTA, meaning the GBP contact area was approximately 1.8 times higher than the average ballast block.

Pressure distribution tests

The collection of representative MBTSS data provides a comparison of qualitative pressure distribution characteristics from each support condition (Fig. 7). The polyurethane foam UTP was more conformal to

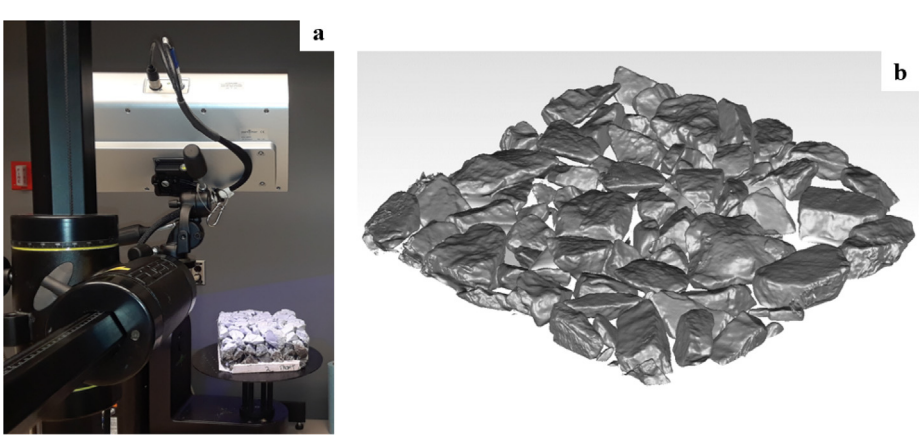

Fig. 4. 3D scanning setup (a) and finished scan of a ballast block (b).

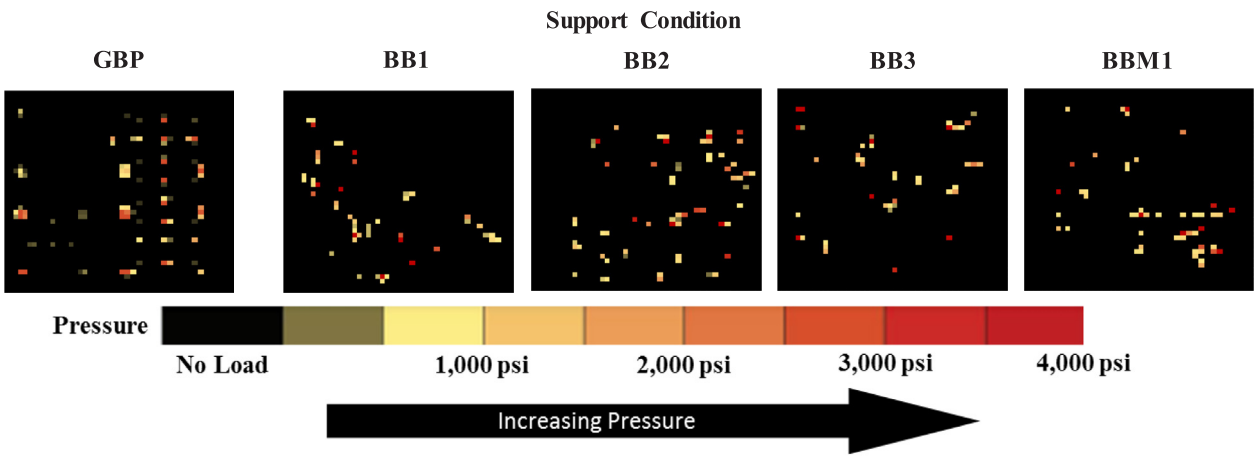

(a)

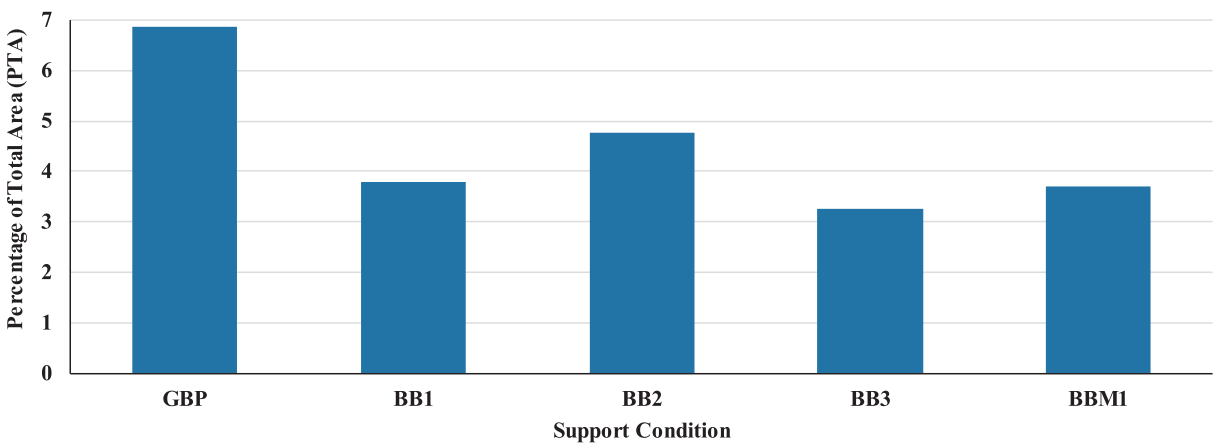

(b)

Fig. 6. Contact distribution for different support conditions from top surface contact tests (a) and top surface contact area as percentage of total sample area (b).

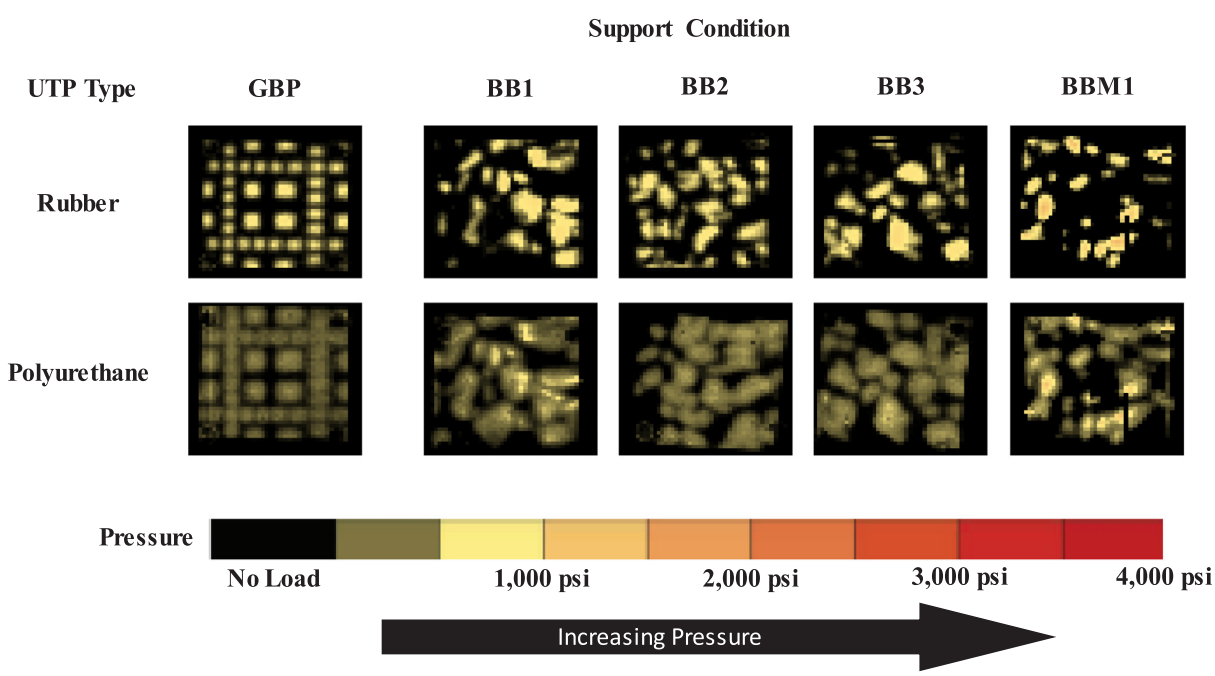

Fig. 7. Pressure distribution of rubber and polyurethane UTPs over different support conditions.

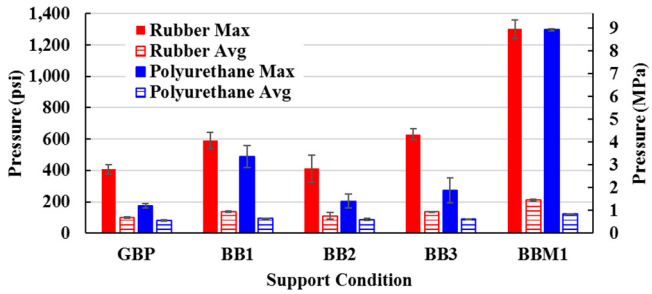

Fig. 8. Mean maximum and average pressure results for each UTP type on each support condition.

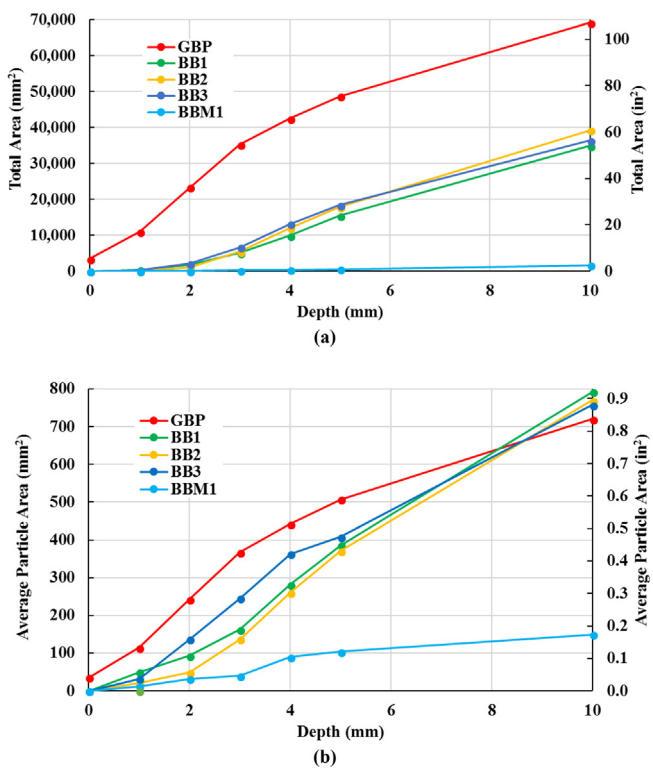

Fig. 9. Total area (a) and average particle area (b) for each support condition at corresponding depths.

Table 1
Total contact area for each support condition at various depths.

		Depth						
	mm²	0	1	2	3	4	5	10
	in²		*0.04*	*0.08*	*0.12*	*0.16*	*0.20*	*0.39*
GBP	mm²	3382	11,018	23,297	35,252	42,498	48,670	69,136
	in²	*5.2*	*17.1*	*36.1*	*54.6*	*65.9*	*75.4*	*107.2*
Standard Block Avg.	mm²	0	207	1602	5714	11641	17,223	36,835
	in²	*0*	*0.3*	*2.5*	*8.9*	*18.0*	*26.7*	*57.1*
BBM1	mm²	0	37	95	198	359	521	1641
	in²	*0*	*0.1*	*0.1*	*0.3*	*0.6*	*0.8*	*2.5*

the surface of the support condition under load than the rubber UTP and therefore exhibited evidence of greater contact and consequent lower pressure magnitudes. The qualitative data presented in Fig. 7 shows similar trends of pressure distribution between both types of support conditions. While the total contact area appears to be similar, the size of the ballast particles varies extensively for the ballast blocks while remaining consistent for the GBP, as expected. For a majority of

Table 2
Average particle area for each support condition at various depths.

		Depth						
	mm²	0	1	2	3	4	5	10
	in²		*0.04*	*0.08*	*0.12*	*0.16*	*0.20*	*0.39*
GBP	mm²	35.2	114.8	242.7	367.2	442.7	507.0	720.0
	in²	*0.1*	*0.2*	*0.4*	*0.6*	*0.7*	*0.8*	*1.1*
Standard Block Avg.	mm²	0	33.8	93.1	181.7	301.9	388.8	773.4
	in²	*0*	*0.1*	*0.1*	*0.3*	*0.5*	*0.6*	*1.2*
BBM1	mm²	0	12.2	31.5	39.7	89.6	104.3	149.2
	in²	*0*	*0.0*	*0.0*	*0.1*	*0.1*	*0.2*	*0.2*

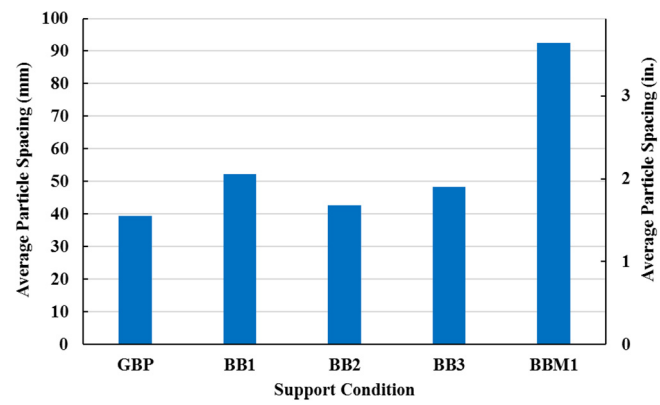

Fig. 10. Average particle spacing by support condition.

the loaded sensels, the pressures seem consistent between the GBP and the ballast blocks. However, the ballast blocks, particularly BBM1, do exhibit points of larger pressures. This is likely a result of sharper points of contact and less overall contact area at the interface between the ballast and UTP sample leading to higher pressure concentrations at these points.

The maximum and average pressure results from the pressure distribution tests are shown in Fig. 8. From this figure, it is apparent that the GBP yields lower values for both maximum and average pressures than all four ballast blocks. When comparing the combined mean data from all ballast blocks against the GBP, the ballast blocks resulted in 1.5 and 3.2 times higher maximum pressure than the GBP for the rubber and polyurethane UTPs, respectively. When removing BBM1 from the mean data and considering only the standard blocks, results show 1.3 and 1.8 times higher maximum pressures than the GBP. This indicates that the pressure demand on UTPs is higher when using actual ballast particles when compared to the GBP. This furthers the evidence that the GBP does not fully represent the true contact characteristics of ballast.

3D Scanning

The total area occupied by each support condition at depths between 1 and 5 mm (0.04 and 0.2 in.) and 10 mm (0.4 in.) were determined for each block using the contour plots generated from the 3D scan data (Fig. 9(a) and Table 1). For all blocks, the total areas at all depths were less than the area occupied by the GBP. For example, the GBP exhibited roughly 2 and 3 times higher areas than the standard blocks at depths of 5 and 10 mm (0.2 and 0.4 in.), respectively. BBM1, the block modified to represent an uneven contact surface, resulted in substantially less area than the GBP with 93 and 42 times less area at 5 and 10 mm (0.2 and 0.4 in.), respectively. This metric is critical for resilient components that deflect/conform as loads are applied and have a tendency to penetrate into the voids around the ballast particles. Since the GBP resulted in higher surface areas at all depths, these components are more likely to exhibit lower pressures, resulting in a less severe and less representative condition when compared to ballast.

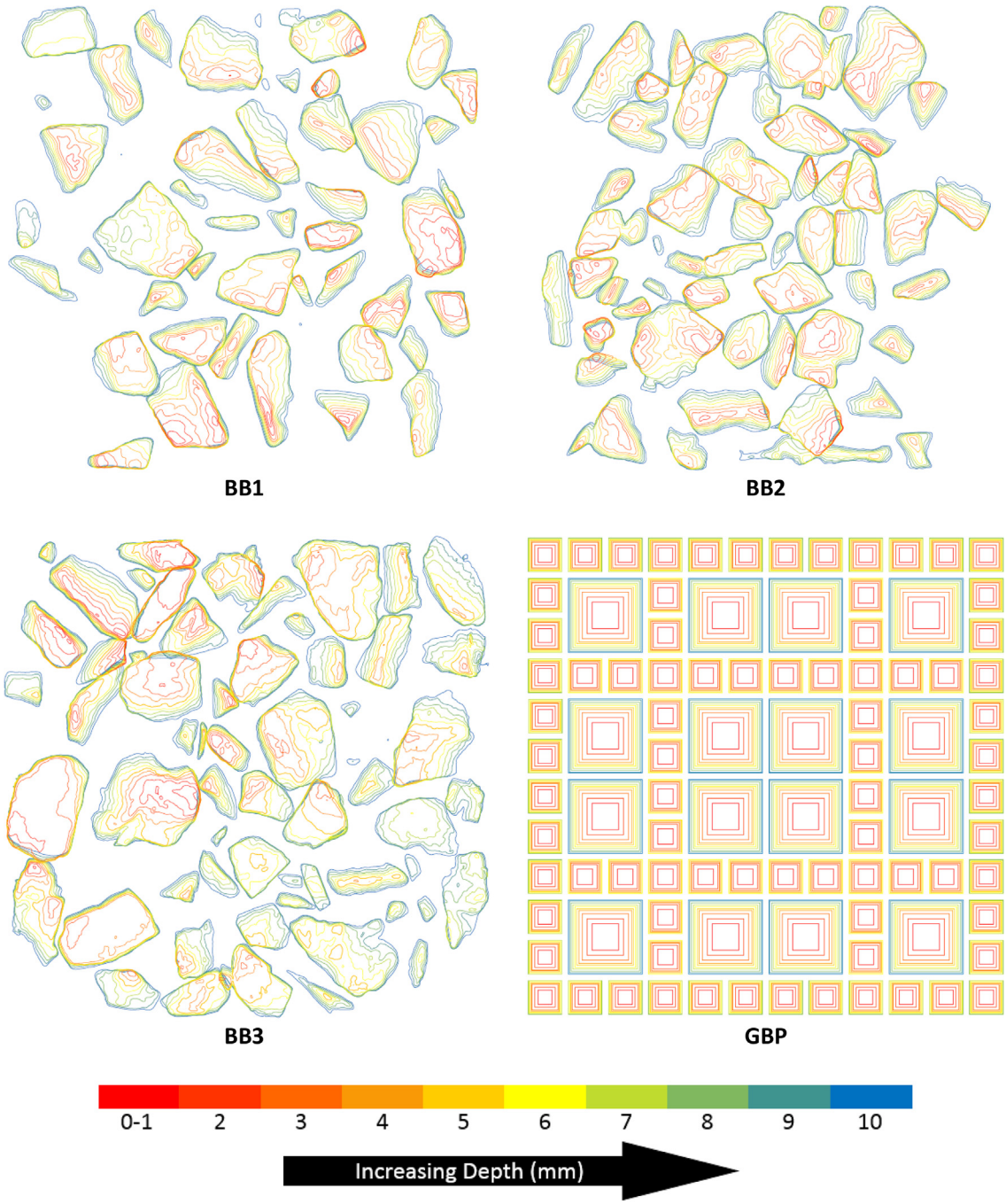

Fig. 11. Contour maps of ballast blocks with lines ranging from 0 to 10 mm (0.4 in.).

The scan data also enabled average particle size per elevation per block to be determined for depths between 0 and 10 mm (0.2 and 0.8 in.) based on the number of particles (or nodes in the case of the GBP) present at each depth (Fig. 9(b) and Table 2). The results show that the GBP, as expected, has a higher average particle area than all ballast blocks at all shallower elevations. At 5 mm (0.4 in.), the GBP exhibits around 1.3 and 4.9 times higher average particle areas than the average standard ballast block and modified block, respectively. Therefore, the nodes in the GBP at these depths are larger than the average ballast particle and consequently provide better support during testing. At elevations greater than 8 mm (0.31 in.) however, the standard ballast blocks yield slightly higher average particle areas than the GBP, approximately 1.1 times higher at 10 mm (0.4 in.). While this result indicates that the GBP provides less ideal support at deeper depths, areas at depths greater than 8 mm (0.31 in.) are only applicable for components that have a tendency to deform heavily as load is applied. Further analysis of the distributions of average particle area data indicates that the GBP node areas are comparable to some of the ballast particles at each depth. However, the ballast blocks have greater variability in particle areas, particularly with particles that are smaller than the GBP. With only three fixed node sizes, the GBP does not adequately represent the variability of particle areas that exist in real ballast.

The spacing of nodes on the GBP was also closer than the particle spacing on all four of the ballast blocks (Fig. 10). Particles in the standard blocks were spaced 1.1 to 1.3 times farther apart on average than the nodes on the GBP. Since very few particles rose to over 5 mm (0.2 in.) on the modified block, the average particle spacing for BBM1 was approximately twice the GBP's average node spacing. In all cases,

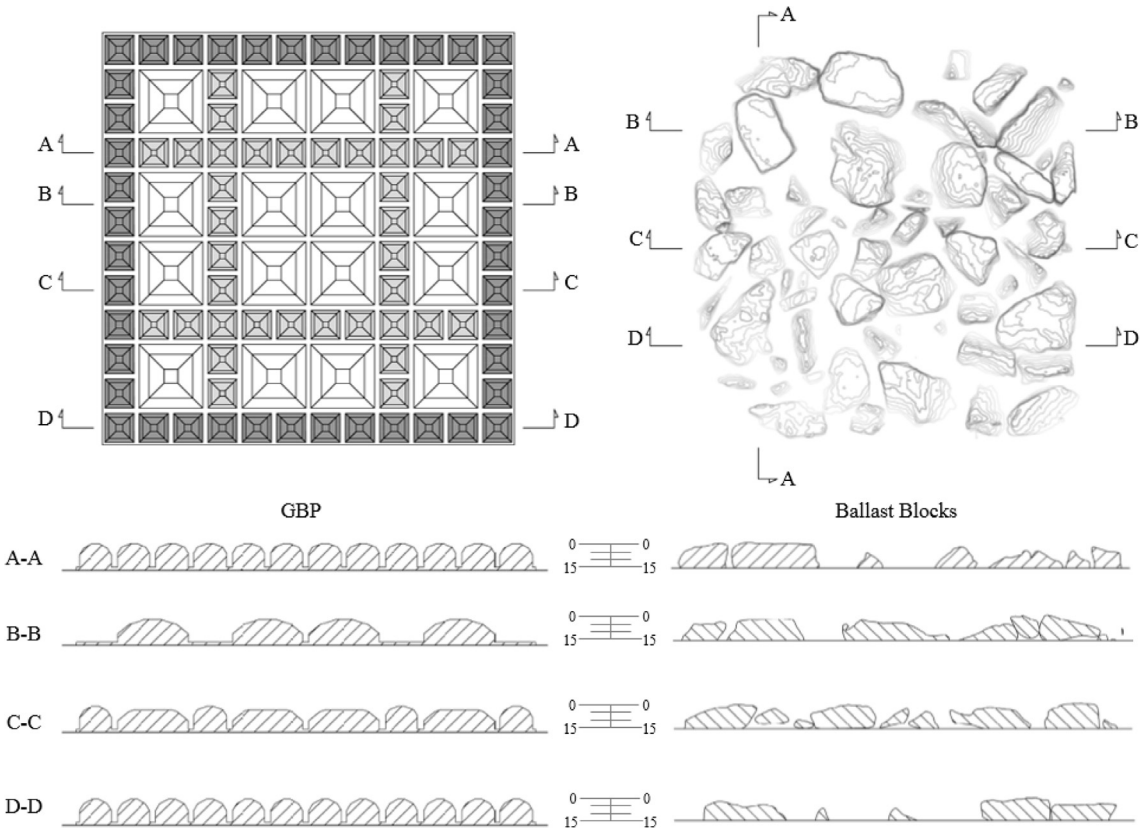

Fig. 12. Representative cross sectional comparison between GBP and BB3.

the GBP provides a more even distribution and less opportunity for component tearing than the ballast blocks due to smaller particle spacing. A Z statistical test performed at $\alpha = 0.05$ on all spacing distances indicates that the GBP and standard ballast blocks have statistically significant different average particle spacing, again showing that the GBP does not accurately represent the ballast interface.

From the 3D scan data, contour plots were compiled for visual comparison of the ballast blocks and the GBP (Fig. 11). Similar trends to what has already been stated are noticeable from the standard blocks with each block showing a similar number of particles and consistent coloring of their contour lines. This indicates that these blocks are representative of a good support condition with similar elevations for each individual particle. Overall, the GBP shows a more consistent pattern than the standard blocks with higher contour lines visible on all nodes, indicating more contact area at shallower depths. This is consistent with the findings of area at each of the depths discussed previously. BBM1 has been omitted due to space constraints.

Four representative cross sections were also selected from the GBP and BB3 to examine the angularity and contact surface of each support condition (Fig. 12). Special care was taken for both conditions to select cross sections that contained several particle peaks. These cross sections are displayed at depths between 0 and 15 mm (0.6 in.) to demonstrate how the full nodes of the GBP correspond to individual ballast particles. Consistent with findings from the average particle area results, the cross sections show that the nodes on the GBP do replicate some particles on the blocks, particularly particles with flat top surfaces. However, factors other than average particle area, such as sharp top points on some of the ballast particles, are not replicated by any of the three node designs on the GBP. Furthermore, these cross sections show variability in height within the ballast with some particles rising higher than others. The GBP, with a consistent top height for all nodes, does not accurately represent this detail. Thus, while average particle area is similar between the two support conditions, differences do exist between ballast particles and the nodes of the GBP.

Conclusions

Results from both the top surface contact tests and pressure distribution tests indicate that the GBP yielded less severe contact properties than ballast. These findings were reinforced by the data from the 3D scans. Results from the top surface contact tests and pressure distribution tests compared favorably to the work of Grabe et al. [9], which studied UTP characteristics on unbonded ballast. The following summarizes the findings of this research:

- Top surface contact test results showed that the GBP exhibited 1.8 times more contact area compared to the average of the standard ballast blocks.
- Pressure tests with UTP samples showed that the GBP exhibited 1.5 and 3.2 times lower contact pressure compared to the ballast blocks using the rubber and polyurethane, respectively.
- Total particle area calculated for the GBP was roughly 3 times the area of the standard blocks at 5 mm (0.2 and 0.4 in.)
- Average particle areas at depths shallower than 8 mm (0.3 in.) were higher for the GBP than all blocks, resulting in more overall contact for conformal specimens during testing. However, the standard ballast blocks had higher average particle areas at deeper depths.
- Average particle spacing for the GBP was between 1.1 and 1.3 times higher than the standard blocks, indicating the GBP has more points of contact and more even distribution than what is found in real ballast.
- When comparing cross section profiles, the GBP has mixed results replicating ballast particles, with some resemblance between the nodes and particles with flatter top surfaces and little resemblance between nodes and particles with sharper top edges.

Taken as a whole, the results from this paper present findings that the GBP overestimates the contact characteristics of well-maintained ballast in railroad tracks, therefore reducing the severity during testing. For all metrics analyzed within this paper, the GBP performed more favorably than both the standard ballast blocks representing well-supported conditions and the modified block representing more severe support conditions. To ensure representative results from laboratory testing of resilient track components, the findings from this research should be considered when designing a more-representative test support condition to be used in North America. This will enable testing conditions that are both efficient and realistic to real-world applications.

Declarations of Interest

None.

Acknowledgements

This research has been primarily supported through funding from the National University Rail Center (NIURail). The positions presented within this paper represent those of the authors and not necessarily those of NURail. Laboratory experimentation for this paper was performed at the Research and Innovation Laboratory (RAIL) at the Harry Schnabel, Jr. Geotechnical Laboratory in Champaign, IL. The loading frame utilized for this testing is owned by Progress Rail Services Corporation, a Caterpillar Company. Epoxy used in the construction of ballast blocks was provided by BASF Corporation.

The authors confirm contribution to the paper as follows: study conception and design: Jacob M. Branson, Marcus S. Dersch, and Arthur de Oliveira Lima; data collection: Jacob M. Branson and Jae-Yoon Kim; analysis and interpretation of results: Jacob M. Branson, Marcus S. Dersch, Arthur de Oliveira Lima, J. Riley Edwards, and Jae-Yoon Kim; draft manuscript preparation: Jacob M. Branson, Marcus Dersch, Arthur de Oliveira Lima, and J. Riley Edwards. All authors reviewed the results and approved the final version of the manuscript.

Funding: This work was supported by the Progress Rail Services Corporation and the National University Rail (NURail) Center, a USDOT-OST Tier 1 University Transportation Center. Jacob M. Branson, Marcus S. Dersch, and Arthur de Oliveira Lima were partially funded by Progress Rail Services Corporation. Riley Edwards has been funded in part through grants to the UIUC Rail Transportation and Engineering Center (RailTEC) from CN and Hanson Professional Services.

References

[1] American Railway Engineering and Maintenance-of-Way Association (AREMA). Manual for railway engineering. Lanham, MD: The American Railway Engineering and Maintenance-of-Way Association; 2016.
[2] Boler H. On the shear strength of polyurethane coated railroad ballast[master's thesis]. Urbana (IL): University of Illinois at Urbana-Champaign; 2012.
[3] Chew PL. Constrained Delaunay triangulations. Algorithmica 1989;4:97–108.
[4] Dersch MS, Tutumluer E, Peeler CT, Bower DK. Polyurethane coating of railroad ballast aggregate for improved performance. Proceedings of the 2010 Joint Rail Conference, Urbana, IL. 2010.
[5] Devrim A, Grun A, Breuckmann B, Lahanier C. High definition 3D-scanning of arts objects and paintings. Structured light and laser scanning, Zurich, CH. 2007. p. 50–8.
[6] DIN 45673-5 Mechanical vibration - Resilient elements used in railway tracks - Part 5: Laboratory test procedures for under-ballast mats. Deutsches Institut fur Normung, Berlin, DE; 2010.
[7] EN 16730:2016 Railway applications - Track - Concrete sleepers and bearers. European Committee for Standardization; 2016.
[8] Fortune S. Voronoi diagrams and Delaunay triangulations; 1995.
[9] Grabe PJ, Mtshotana BF, Sebati MM, Thunemann EQ. The effects of under-sleeper pads on sleeper-ballast interaction. J South Afr Inst Civil Eng. 2016;58(2):35–41.
[10] Greve MJ, Dersch MS, Edwards JR, Barkan CPL, Thompson H, Sussmann TR, et al. Examination of the effect of concrete crosstie rail seat deterioration on rail seat load distribution. Transp Res Rec 2015;2476:1–7.
[11] Greve MJ, Dersch MS, Edwards JR, Barkan CPL, Mediavilla J, Wilson BM. The effect of particle intrusion on rail seat load distributions on heavy haul freight railroads. Proceedings of the 2015 International Heavy Haul Conference, Perth, AT. 2015.
[12] Indraratna B, Nimbalkar S, Navaratnarajah SK, Rujikiatkamjorn C, Neville T. Use of shock mats for mitigating degradation of railroad ballast. Sri Lankan Geotech J – Special Issue Ground Improv 2014;6(1):32–41.
[13] Johansson A, Nielsen JCO, Bolmsvik R, Karlstrom A, Lunden R. Under sleeper pads—Influence on dynamic train-track interaction. Wear 2008;265:1479–87.
[14] Kaewunruen S, Remennikov AM. Under sleeper pads: field investigation of their role in detrimental impact mitigation. Proceedings of the 13th international railway engineering conference, Edinburgh, UK. 2015. p. 1–17.
[15] Lakusic S, Ahac M, Haladin I. Experimental investigation of railway track with under sleeper pad. Slovenski Kongres O Cestah In Prometu, Portoroz, RS. 2010.
[16] Lima A de O, Dersch MS, Edwards JR, Tutumluer E. Laboratory Study into the effect of support condition on ballast mat bedding modulus and insertion loss. Transport Res Rec 2017;2476:23–31.
[17] Lima A de O, Dersch MS, Qian Y, Tutumluer E, Edwards JR. Laboratory mechanical fatigue performance of under-ballast mats subjected to North American loading conditions. Proceedings of 11th International Heavy Haul Association Conference, Cape Town, ZA. 2017.
[18] Lima A de O. Under ballast mats for railway infrastructure–a North American approach to component characterization [master's thesis]. Urbana (IL): University of Illinois at Urbana-Champaign; 2017.
[19] Loy H. Mitigating vibration using under-sleeper pads. Railway Gazette Int 2012:40–2.
[20] McHenry MT, Brown M, LoPresti J, Rose J, Souleyrette R. The use of matrix based tactile surface sensors to assess the fine scale ballast-tie interface pressure distribution in railroad track. Transp Res Rec 2015;2476:23–31.
[21] Merheb A, Loy H, Marcos J, Oliveira L, Bernucci L. Improvement of sleeper-ballast contact using under sleeper pads in heavy haul lines. Proceedings of the GEORAIL 2017 International Symposium, Paris, FR. 2017.
[22] Rapp CT, Edwards JR, Dersch MS, Barkan CPL, Mediavilla J, Wilson BM. Measuring concrete crosstie rail sear pressure distribution with matrix based tactile surface sensors. Proceedings of the 2012 Joint Rail Conference, Philadelphia, PA. 2012.
[23] Rose JG, Stith JC. Pressure measurements in railroad trackbeds at the rail/tie interface using tekscan sensors. Proceedings of the American Railway Engineering and Maintenance of Way Association Conference, Nashville, TN. 2004.
[24] Schilder R. USP (Under Sleeper Pads) – a contribution to save money in track maintenance. Proceedings of AusRAIL PLUS 2013, Sydney, AT. 2013.
[25] Selig ET, Yoo TS, Panuccio CM. Mechanics of ballast compaction volume 2: field methods for ballast physical state measurement. Washington, DC: Federal Railroad Administration; 1982.
[26] Stith JC. Railroad track pressure measurements at the rail/tie interface using Tekscan sensors [master's thesis]. Lexington (KY): University of Kentucky; 2005.

Jacob Branson is an MS student in civil engineering at the University of Illinois at Urbana-Champaign (UIUC). He graduated from the University of Missouri-St. Louis/Washington University Joint Engineering Program with a BS in Civil Engineering in 2017. He worked as an engineering consultant during undergraduate studies focusing on rail project design and construction. His research interests include railroad infrastructure components with a specific focus on resilient materials.

Marcus Dersch is a Senior Research Engineer at the University of Illinois at Urbana-Champaign (UIUC). He obtained his Bachelors and Masters degrees in Civil Engineering from UIUC in 2009 and 2010 respectively, during which time he completed research in Railroad Engineering focusing on railroad ballast performance. He worked for Union Pacific Railroad as an engineering intern in 2008 and joined the Rail Transportation and Engineering Center at UIUC in 2011. He obtained his Professional Engineer's License in 2015 and his current research interest is railway infrastructure design and performance with a focus on sleepers, fasteners, and railroad ballast.

Arthur de Oliveira Lima obtained his BS in Civil Engineering in 2015 from the Federal University of Vicosa in Brazil with a portion of his studies conducted at the University of Waterloo in Canada where he was involved with research into concrete pavement materials and durability. He obtained his MS in Civil Engineering at the University of Illinois at Urbana-Champaign focusing on railroad infrastructure research. He currently serves as an Experimentation Engineer with RailTEC at the University of Illinois at Urbana-Champaign where he helps manage rail infrastructure research. Mr. Lima is a member of AREMA Committee 30 – Ties and of the APTA Track/Noise and Vibration Technical Forum and his research interests involve all aspects of rail civil infrastructure, from either the materials, components, or structures perspective.

J. Riley Edwards is a Senior Lecturer and Research Scientist in the Rail Transportation and Engineering Center (RailTEC) at the University of Illinois at Urbana-Champaign (UIUC), where he oversees rail infrastructure research and advises students. He obtained his BS in Civil Engineering from Vanderbilt University in 2004 and a MS from UIUC in 2006. After graduation, he worked for Hanson Professional Services, Inc. as a Construction Engineer on BNSF Railway's Memphis Intermodal Expansion project in Tennessee. His research interests include the design and performance of railway track components.

Jae-Yoon Kim is a master's student in Civil Engineering at the University of Illinois at Urbana-Champaign (UIUC). He serves as a Graduate Research Assistant with the Rail Transportation and Engineering Center at UIUC. He obtained his bachelor's degree in Civil Engineering from the University of Seoul in 2008. He worked as an Assistant Engineer for Samsung Construction & Trading Corporation where he was involved in road and metro projects from 2008 to 2016. His current research interest is an investigation of timber crosstie spike failure.